Image transmission using stable solitons of arbitrary shapes in photonic lattices

Jianke Yang,[1,*] Peng Zhang,[2] Masami Yoshihara,[2] Yi Hu,[3] and Zhigang Chen[2,3]

[1]*Department of Mathematics and Statistics, University of Vermont, Burlington, Vermont 05401, USA*

[2]*Department of Physics and Astronomy, San Francisco State University, San Francisco, California 94132, USA*

[3]*TEDA Applied Physics School, Nankai University, Tianjin 300457, China*

**Corresponding author: jyang@math.uvm.edu*

Received November 10, 2010; accepted January 17, 2011;
posted February 4, 2011 (Doc. ID 138034); published March 1, 2011

We demonstrate both theoretically and experimentally that photonic lattices under self-defocusing nonlinearity support gap solitons in various shapes such as cross and H shapes. These solitons, with their intensity humps all in-phase, are stable against perturbations, thus they propagate robustly throughout the lattices. Based on this finding, we propose soliton-based text/image transmission through bulk photonic structures. © 2011 Optical Society of America

OCIS codes: 190.0190, 160.5293.

Image transmission through bulk nonlinear media is a challenging problem due to heavy nonlinear distortions. Several techniques have been demonstrated, including image transmission based on phase conjugation [1], incoherent soliton waveguides [2], and digital holography [3]. Recently, image transmission based on coherent destruction of tunneling has also been demonstrated [4,5]. Despite these techniques, transmission of sophisticated images with high fidelity is still very difficult. Recent progress in photonic-lattice research reveals some new phenomena in self-defocusing nonlinear media. In particular, it was found that nonlinear Bloch states in photonic lattices can be truncated to form stable soliton clusters with an arbitrary number of adjacent intensity humps [6,7]. Stimulated by such phenomena, we show in this Letter that in a photonic lattice under self-defocusing nonlinearity, one can construct stable gap solitons whose intensity humps can form almost arbitrary shapes (such as cross and H shapes), and these humps are all in-phase with each other. Based on this finding, we propose to transmit text and images with these solitons through self-defocusing photonic lattices, and to demonstrate such transmission both theoretically and experimentally.

The theoretical model we use for light transmission in a self-defocusing photonic lattice is

$$iU_z + U_{xx} + U_{yy} + n(x,y)U - |U|^2U = 0, \qquad (1)$$

where z is the direction of propagation, (x,y) is the transverse coordinate, and $n(x,y)$ is the periodic transverse refractive-index variation. All variables have been normalized. Experimentally, the index variation $n(x,y)$ can be induced by optical induction [8–10], and thus is called optically-induced photonic lattice. In our analysis, we take the lattice to be $n(x,y) = h(\cos^2 x + \cos^2 y)$, where h is the index-variation depth parameter. This lattice is shown in Fig. 1(a). Note that this lattice has periodic index humps and dips, and it closely resembles the "egg-crate" lattice [11] optically induced in our experiment [see Fig. 1(e)]. For simplicity, we use in our theoretical model the cubic (Kerr-type) self-defocusing nonlinearity (in our experiment, the photorefractive nonlinearity is saturable rather than cubic [8–10], but we have found numerically that both cubic and saturable nonlinearities give qualitatively similar results).

We look for stationary solitons in Eq. (1) in the form $U(x,y,z) = u(x,y)e^{-i\mu z}$, where $u(x,y)$ is a real-valued localized function, and μ is the propagation constant. We find that Eq. (1) supports gap solitons of almost arbitrary shapes when the lattice is sufficiently deep. To demonstrate, we take the lattice-depth parameter $h = 6$ as an example. The first two Bloch bands for this lattice are displayed in Fig. 1(d). In the gap between these two bands, solitons with three intensity humps aligned along one of the principal axes of the lattice are found. This soliton at $\mu = 6$ is displayed in Fig. 1(b). These three intensity humps have the same phase, and they are located at three adjacent lattice sites (high-index positions). Using the continuation method, we can obtain the entire family of this gap soliton. The power curve of this family is shown in Fig. 1(d). It is seen that this power curve has double branches, and the soliton in Fig. 1(b) is located on the lower branch. On the upper branch, the soliton in this family develops two extra intensity humps at the edges, and these extra humps are out of phase with the three

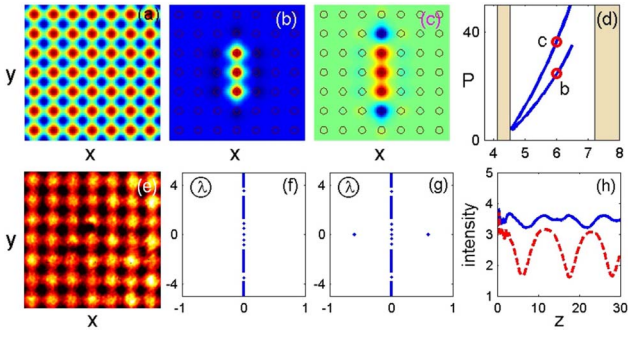

Fig. 1. (Color online) (a), (e) Photonic lattice as used in our theory (a) and experiment (e); (b), (c), (d) line-soliton solutions, where (d) is the power curve, and (b), (c) show soliton profiles at marked points in (d); (f), (g) stability spectra of gap solitons in (b), (c), respectively; (h) stable (solid) and unstable (dashed) evolutions of the top hump's intensity for solitons in (b), (c) under perturbations. Background circles in (b), (c) mark lattice sites. Shaded regions in (d) represent the first two Bloch bands.

humps in the interior. To illustrate this, the soliton at the marked point on the upper branch ($\mu = 6$) is shown in Fig. 1(c). Our important finding is that these gap solitons on the lower branch are linearly stable, while the ones on the upper branch are not. The linear-stability spectra of gap solitons in Figs. 1(b) and 1(c) are displayed in Figs. 1(f) and 1(g), respectively. These spectra are obtained numerically by turning the linear-stability eigenvalue problem of these solitons into a matrix eigenvalue problem through Fourier collocation methods [12]. Note that all eigenvalues in Fig. 1(f) lie on the imaginary axis, indicating that the soliton in Fig. 1(b) is linearly stable. But the spectrum in Fig. 1(g) contains positive eigenvalues, indicating that the soliton in Fig. 1(c) is linearly unstable.

The above linear-stability results are corroborated by nonlinear evolution simulations of these gap solitons under perturbations. For the lower-branch gap soliton in Fig. 1(b), we have added various random-noise perturbations, and found that the perturbed soliton can always transmit stably for arbitrarily long distances if the initial perturbation is not too strong. For instance, for one realization of 10% random-noise perturbations, the intensity of the top hump in this soliton versus distance z is displayed in Fig. 1(h) (solid curve). One can see only small intensity oscillation around its initial value. The same holds for the other two humps in this soliton. Thus this soliton in Fig. 1(b) is nonlinearly stable, in agreement with the linear stability of this soliton shown in Fig. 1(f). However, when the upper-branch soliton in Fig. 1(c) is perturbed by the same amount of noise, the intensities of its five humps can move far away from their initial values [see Fig. 1(h), dashed curve). Note that this intensity can decrease by over 50% from its initial value, leading to breakdown of the soliton structure. Thus this soliton is nonlinearly unstable, again in agreement with its linear instability shown in Fig. 1(g).

The above stability property can be heuristically understood. It has been shown that in a lattice under defocusing nonlinearity, a dipole soliton is stable if its two humps residing in adjacent lattice sites are in-phase, but unstable otherwise [12–14]. Thus, line gap solitons composed of all in-phase intensity humps [as in Fig. 1(b)] are expected to be stable, whereas those containing out-of-phase intensity humps [as in Fig. 1(c)] are unstable.

An important finding in this Letter is that, in addition to the family of line-shape gap solitons in Fig. 1, the lattice also supports gap solitons in almost arbitrary configurations. As examples, three other gap solitons at $h = 6$ and $\mu = 6$ are shown in Figs. 2(a)–2(c). The soliton in Fig. 2(a) has three intensity humps forming a 90° corner; the soliton in Fig. 2(b) has nine intensity humps forming a cross shape, and the soliton in Fig. 2(c) has 12 intensity humps forming an H-shape. All intensity humps in these solitons have the same phase, and are located at lattice sites. Note that the shapes of these solitons are much more general and flexible than the truncated-Bloch-wave solitons reported in [6]. Intuitively, the existence of these solitons of arbitrary shapes can be understood by viewing the line soliton of Fig. 1(b), the corner soliton of Fig. 2(a), and the in-phase dipole soliton [12–14] as building blocks. Using these basic blocks, one can construct arbitrary shapes of solitons. An important fact is that all these solitons of various shapes are linearly and nonlinearly stable, just like the line soliton in Fig. 1(b). For instance, the stability spectrum of the H-shaped soliton in Fig. 2(c) is shown in Fig. 2(d). It is seen that all the eigenvalues in this spectrum lie on the imaginary axis, indicating that this soliton is linearly stable. Our numerical simulation of this soliton under perturbations shows that this soliton is nonlinearly stable as well. This stable behavior agrees with our earlier intuition that under defocusing nonlinearity, adjacent in-phase intensity humps form stable structures.

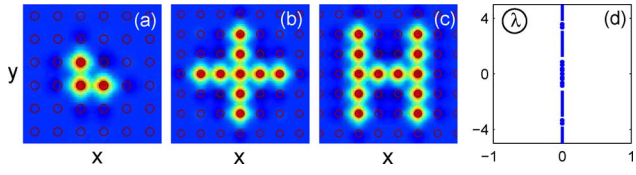

Fig. 2. (Color online) (a)–(c) Three gap solitons of different shapes obtained at $h = 6$ and $\mu = 6$; (d) stability spectrum of the H-shaped soliton in (c).

The various solitons in Fig. 2 were obtained at a particular propagation constant μ. When μ varies (with the lattice unchanged), each of these solitons will generate its own solution family. The power curve of each solution family has double branches, just as in Fig. 1(d). The stable in-phase solitons in Fig. 2 all lie on the lower branches of the respective families. Unstable solitons on the upper branches develop additional out-of-phase intensity humps, similar to Fig. 1(c).

The above stable solitons can be used for text and image transmission. To demonstrate the principle, we performed experiments in a biased photorefractive SBN:60 crystal with the optical induction technique [8–10]. First, a two-dimensional ionic-type lattice [11] with spacing 28 μm is created with an ordinarily polarized lattice-inducing beam, which propagates invariantly throughout the 10-mm-long crystal at a negative bias field of −1.4 kV/cm (hence the nonlinearity is self-defocusing). This ionic lattice was formed by interfering two pairs of beams, with one pair out of phase, and the other pair in phase. The output of this lattice is shown in Fig. 1(e), which resembles the lattice in our theoretical model [see Fig. 1(a)]. Then an extraordinarily polarized probe beam is sent through an amplitude mask to form the desired cross or H shape [Fig. 3(a)] at the input to the crystal.

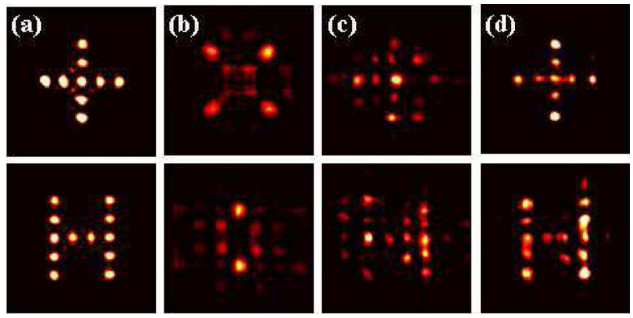

Fig. 3. (Color online) Experimental results on image transmission in photonic lattice [shown in Fig. 1(e)] under self-defocusing nonlinearity: (a) input pattern, (b) linear output without lattice, (c) linear output with lattice, (d) nonlinear output with lattice.

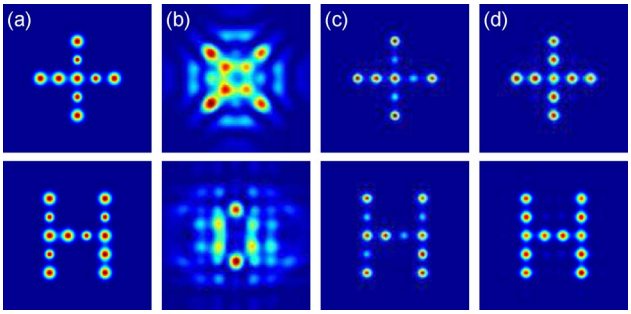

Fig. 4. (Color online) Simulations corresponding to experiments of Fig. 3: (a) input; (b), (c) linear outputs without and with lattice; (d) nonlinear output with lattice.

Without the induced lattice, linear propagation of the probe beam leads to strong diffraction and deformation of the initial shape at the crystal output [Fig. 3(b)]. With the induced lattice at the bias field of −1.4 kV/cm, linear propagation of the probe beam experiences discrete diffraction so that the input patterns also are distorted due to waveguide coupling among lattice sites [Fig. 3(c)]. However, nonlinear propagation of the probe beam leads to self-trapping of gap soliton clusters in the shape of the input pattern [Fig. 3(d)]. Thus, soliton-based transmission of cross or H shape is established in the nonlinear crystal.

To corroborate these experimental results, we also performed numerical simulations using the theoretical model in Eq. (1) with $h = 6$. Our initial condition is a superposition of Gaussian humps forming a cross or H pattern [Fig. 4(a)], and all humps are located at lattice sites. The peak intensities of these Gaussian humps are all equal to each other (at 3.2), but their widths are slightly varied to mimic the experimental initial conditions in Fig. 3. The simulation distance is $z = 2.2$, which corresponds to the crystal length in the experiment. The simulation results are shown in Fig. 4. Clearly, these results agree well with experimental results in Fig. 3. In particular, these results show that the initial cross and H patterns hold up much better in the lattice with defocusing nonlinearity [Fig. 4(d)] than without nonlinearity [Fig. 4(c)] or without lattice [Fig. 4(b)]. We have performed simulations to longer distances as well and found that, in the lattice under defocusing nonlinearity, cross and H patterns show little distortion for all distances. Comparatively, without the nonlinearity and/or the lattice, these patterns further distort from their original shapes and totally break up at longer distances.

We would like to point out that when the nonlinearity is self-focusing [i.e., the nonlinear coefficient in Eq. (1) is positive], we have found stable solitons of arbitrary shapes as well. The main difference from the defocusing case is that intensity humps in these stable solitons are now out of phase with each other. This phenomenon can also be exploited for image transmission, but intensity humps (pixels) in these images now need to be phase-engineered so that neighboring pixels are out of phase with each other.

In summary, we have theoretically and experimentally demonstrated that photonic lattices support stable gap solitons of almost arbitrary shapes. We expect that this phenomenon can be utilized as a new way for image transmission through nonlinear media.

This work was supported by the National Science Foundation (NSF), Air Force Office of Scientific Research (AFOSR) and the 973 Program of China.

References

1. A. Yariv, Opt. Commun. **21**, 49 (1977).
2. D. Kip, C. Anastassiou, E. Eugenieva, D. Christodoulides, and M. Segev, Opt. Lett. **26**, 524 (2001).
3. C. Barsi, W. Wan, and J. W. Fleischer, Nat. Photon. **3**, 211 (2009).
4. Y. V. Kartashov, A. Szameit, V. A. Vysloukh, and L. Torner, Opt. Lett. **34**, 2906 (2009).
5. P. Zhang, N. K. Efremidis, A. Miller, Y. Hu, and Z. Chen, Opt. Lett. **35**, 3252 (2010).
6. T. J. Alexander, E. A. Ostrovskaya, and Y. S. Kivshar, Phys. Rev. Lett. **96**, 040401 (2006).
7. J. Wang, J. Yang, T. J. Alexander, and Y. S. Kivshar, Phys. Rev. A **79**, 043610 (2009).
8. J. W. Fleischer, M. Segev, N. K. Efremidis, and D. N. Christodoulides, Nature **422**, 147 (2003).
9. H. Martin, E. D. Eugenieva, Z. Chen, and D. N. Christodoulides, Phys. Rev. Lett. **92**, 123902 (2004).
10. C. Lou, X. Wang, J. Xu, Z. Chen, and J. Yang, Phys. Rev. Lett. **98**, 213903 (2007).
11. P. Zhang, S. Liu, C. Lou, F. Xiao, X. Wang, J. Zhao, J. Xu, and Z. Chen, Phys. Rev. A **81**, 041801(R) (2010).
12. J. Yang, *Nonlinear Waves in Integrable and Nonintegrable Systems* (SIAM, 2010).
13. L. Tang, C. Lou, X. Wang, D. Song, X. Chen, J. Xu, Z. Chen, H. Susanto, K. Law, and P. G. Kevrekidis, Opt. Lett. **32**, 3011 (2007).
14. E. Smirnov, C. E. Rüter, D. Kip, Y. V. Kartashov, and L. Torner, Opt. Lett. **32**, 1950 (2007).